Electronic structure and phase-stability studies on superconducting YNi_2B_2C, YRh_3B, and nonsuperconducting YNi_4B

P. Ravindran
Department of Physics, Anna University, Madras 600 025, India

S. Sankaralingam
Department of Physics, AGGAC, Tindivanam 604 002, India

R. Asokamani
Department of Physics, Anna University, Madras 600 025, India

(Received 9 June 1995)

The band structure and the density of states (DOS) of YNi_2B_2C, YRh_3B, and YNi_4B are obtained using the tight-binding linear muffin-tin orbital method. From our studies, we have found that the Fermi level falls on one of the peaks in the DOS curves of both YNi_2B_2C and YRh_3B and this is responsible for superconductivity in these compounds. In order to comprehend the phase stability of these superconducting materials, the total-energy curves are drawn. The angular momentum and site decomposed DOS studies on paramagnetic YNi_4B clearly show that the nickel d states are partially filled. The equilibrium lattice constants, cohesive energy, heat of formation, density of states at the Fermi level, Pauli paramagnetic susceptibility, electronic specific-heat coefficient, the electron-phonon coupling constant, and the bulk modulus and its pressure derivative are tabulated and compared with the available experimental values.

I. INTRODUCTION

Recently a considerable number of superconducting binary, ternary, and quaternary Ni-based systems are reported[1] and as elemental Ni is ferromagnetic, the identification of superconductivity in Ni-based compounds is of high current interest. Because of the discovery of superconductivity in quaternary rare-earth transition-metal borocarbides with the composition RT_2B_2C (R rare earth, T= Ni, Pd, Pt) having transition temperature (T_c) up to 16.6 K,[2] and with mixed phase Y-Pd-B-C having $T_c = 23$ K,[3] considerable theoretical as well as experimental attention has been focused on these borocarbide systems.

Several one-electron band-structure calculations on these borocarbides have been reported.[4–8] All these studies give evidence for the metallic and three-dimensional character of bands in these compounds with the E_F falling on the peak of the density of states at the top of Ni $3d$-dominated bands which include an appreciable rare-earth d state and a small boron, carbon s-p admixture. Recently, Mattheiss, Siegrist, and Cava discussed that the superconducting behavior of R Ni_2B_2C compounds is attributed to an electron-phonon mechanism in which the high-frequency boron a_{1g} optical phonons dynamically modulate the tetrahedral NiB_4 bond angles.[6] Further, from this detailed band-structure studies, it has been observed that a key energy band feature within the Ni-B-C s-p manifold is sensitive to the NiB_4 tetrahedral geometry and the position of this key energy band relative to E_F is mainly responsible for the superconductivity in these compounds.

Sarro *et al.* reported the T_c of a Th-Pd-B-C specimen to be 21.5 K and they were unable to identify the phase which is responsible for superconductivity.[9] The T_c for the specimen of composition $YPd_5B_3C_{0.35}$ was reported to be 23 K and here also the superconducting phase was not yet identified.[3] The stability of intermetallic compounds has been very much sensitive to the presence of impurities in the starting materials.[10] Hence, the Cu_3Au-type of La_3X (Al, Ga, In, Tl) compounds are found to be metastable and a small addition of carbon stabilizes these compounds.[11] Further, the $LaPt_2B_2C$ compound is found to be in multiphase with the nonstochiometry composition and the addition of Au stabilizes this single-phase material.[6] It is important to note that the stable $ThPd_2B_2C$ is having a lower T_c of 14.5 K than some metastable (unidentified) phase with a T_c of 21.5 K in the Th-Pd-B-C system.[9] Since the physical properties of compounds depend decisively on its crystal structure, the phase-stability studies on these compounds are an urgent task towards the understanding of these materials. As the total-energy is the useful tool to comprehend the structural stability of materials, we have made an attempt to analyze the stability of these compounds through our total-energy studies.

Many ternary borides of rare-earth and transition metals are known to exhibit interesting magnetic and superconducting properties.[12] In particular, many members of RRh_4B_4 series exhibit coexistence of magnetism and superconductivity.[13] In the Y-Rh-B phase diagram, superconductivity with T_c in the range of 1.5 to 11 K has been observed in YRh_6B_4, YRh_3B_2, $YRhB_4$, and YRh_4B_4 systems.[14] Later, the cubic perovskite-type YRh_3B compound with a T_c of 0.76 K was also reported.[15] But Rogl and DeLong argued that the cubic perovskite structure would generally be very unfavorable for the occurrence of superconductivity.[16] Hence, to apprehend the experimentally observed superconductivity in the cubic perovskite YRh_3B, the band-structure

0163-1829/95/52(17)/12921(10)/$06.00

calculations are performed for this system.

The hexagonal intermetallic compounds with $CaCu_5$- type crystal structure possess a variety of interesting ground-state properties. Some of them are newly discovered antiferromagnetic heavy fermion superconductors such as UNi_2Al_3,[17] and UPd_2Al_3,[18] and the permanent magnetic materials like $SmCo_4B$.[19] According to the earlier investigation of the magnetic properties of YNi_4B, which is $CaCu_5$ structural derivative, it has been reported that it is in the paramagnetic state.[20] Further, comparing the susceptibility and specific-heat capacity of YNi_4B with those of closely related system YNi_5, it is suggested that the Ni $3d$ band is filled in YNi_4B (Ref. 21) and thus, the electronic states near Fermi level are mainly of $4d$ character. Moreover, the low-temperature specific-heat and susceptibility measurements show that a small portion of YNi_4B composition is found to be superconducting with T_c of 12 K.[22] It has been believed that the suppression of superstructure in this composition is responsible for its superconductivity.[22] Even though considerable experimental studies are available on YNi_4B system,[20–23] no detailed theoretical studies are made. In order to understand the physical properties of YNi_4B, we have carried out the band-structure and total-energy calculations for this material.

These compounds are chosen for our band-structure studies because these are all yttrium-based boride compounds. Apart from this, of the three systems only YNi_2B_2C and YRh_3B are superconducting and the other is nonsuperconducting. It is interesting to note that the addition of carbon to the nonsuperconducting YNi_4B stabilizes in YNi_2B_2C which is a superconductor with a fairly higher T_c of 16.6 K.

The paper is divided into six sections. The crystal structural aspects and the details of our band-structure calculations are given in Sec. II. Section III deals with the band structure and density of states of the superconducting YNi_2B_2C and YRh_3B and those of the nonsuperconducting YNi_4B. In Sec. IV, the phase stability of these materials from total-energy studies are reported. The equation of states obtained from the total-energy studies for superconducting materials under consideration are given in Sec. V. The important conclusions are presented in the last section.

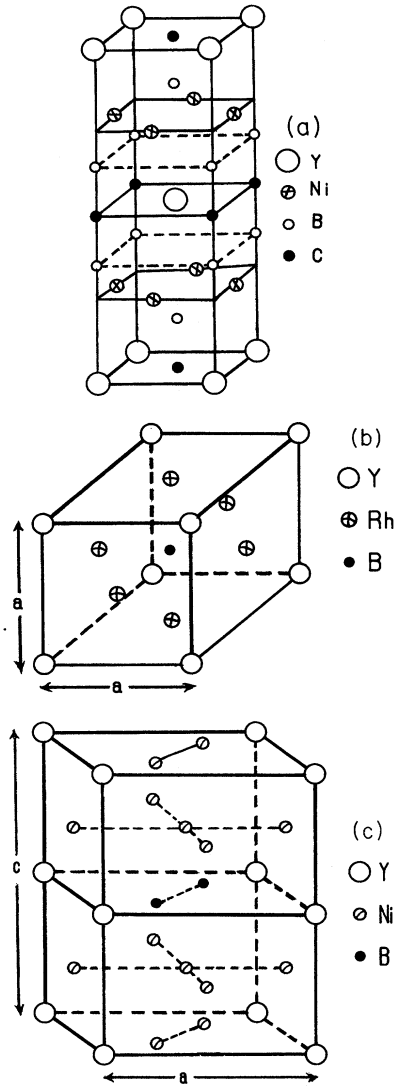

FIG. 1. Crystal structure of (a) YNi_2B_2C, (b) YRh_3B, and (c) YNi_4B.

II. CRYSTAL STRUCTURAL ASPECTS AND THE DETAILS OF CALCULATION

The structure of YNi_2B_2C is body-centered tetragonal (bct) and it can be viewed as a carbon stuffed derivative of $ThCr_2Si_2$ structure (space group $I4/mmm$) in which the carbon atom is located at $2b$ position.[24] It is a fairly simple structure consisting of two-dimensional Ni_2B_2 layers, stacked in the c direction with intervening carbon and yttrium atom as shown in Fig. 1(a). This layering is somewhat reminiscent of the layered high-T_c cuprate superconductors. There are three parameters defining the crystal structure namely the lattice parameters a and c and the parameter $Z=0.353$ determining the position of boron atoms relative to Y and Ni. The NiB_4 tetrahedron, which is formed by Ni atom each of which surrounded by four boron atoms, is believed to be responsible for superconductivity in this compound.

The YRh_3B compound possesses the cubic perovskite structure (space group $Pm3m$) of the $CaTiO_3$ type ($E2_1$) in which Y atom occupies the corners and Rh atoms are located at the faces of the cube.[15] The boron atom occupies the octahedral hole in the center of the Cu_3Au-type unit cell [Fig. 1(b)]. Among the binary superconducting intermetallics, higher-T_c is observed in the $B1$ (NaCl-type) phase of transition-metal carbides or nitrides.[25] The most significant similarity in the structural aspect of the YRh_3B and the $B1$ phase carbides or nitrides is the transition-metal octahedra in which each nonmetal is surrounded by the transition-metal atoms. Further, this octahedral environment is somewhat reminiscent of the high-T_c oxides where the transition metal is surrounded by oxygen.

The crystal structure of YNi_4B is the $CaCu_5$ derivative of the hexagonal $CeCo_4B$-type (space group $P6/mmm$) with the lattice parameters $a=4.9892$ and $c=6.9530$ (Ref. 23) [Fig. 1(c)]. From the structural investigation of YNi_4B single crystal, it has been found that it crystallizes in a superstructure of $CeCo_4B$-type with $a'=3a$ and $c'=c$.[26] However, we have considered only the primitive cell in our calculations.

The primitive cell itself consists of 12 atoms where Ni atoms and Y atoms are in the two distinct positions. Hence, this system is somewhat more complex than the other systems considered here.

In the present study, the self-consistent band structures are presented for the YNi_2B_2C in the bct phase, YRh_3B in cubic structure and YNi_4B in the hexagonal phase within the local-density approximation (LDA) using the scalar relativistic version of tight-binding linear muffin-tin orbital (LMTO) method.[27] The usual local exchange-correlation potential of von Barth and Hedin is used in our band-structure calculations. The band-structure and total-energy calculations are performed within the atomic-sphere approximation[28] (ASA) in which the spheres are permitted to overlap and are expanded until they fill the space and the eigenvalue equation is solved by considering the s, p, and d partial waves only. Apart from this, the combined correction terms,[28] which account for the nonspherical shape of the atomic cells and the truncation of higher partial waves ($l>2$) inside the sphere so as to minimize the errors in the LMTO method, are also included. The tetrahedron method for the Brillouin-zone integrations (i.e., k-space integrations) has been used with its latest version which avoids misweighing and corrects errors due to the linear approximation of the bands inside each tetrahedron.[29]

The electronic configurations in the atomic states of Y ($5s^25p^04d^1$), Rh ($5s^15p^04d^8$), Ni ($4s^24p^03d^8$), B ($2s^22p^13d^0$), and C ($2s^22p^23d^0$) are treated as valence electrons in our calculations. The Wigner-Seitz radius for various constituents are chosen in such a way that the overlap should not exceed 30% which is the permissible limit of ASA. The self-consistency is achieved with an eigenvalue accuracy of 10^{-4} Ry between two consecutive iterations. The eigenvalues are obtained with a set of 105 k points in the irreducible wedge of the first Brillouin zone (IBZ) of the bct lattice for YNi_2B_2C, 84 k points in the IBZ of the cubic lattice for YRh_3B, and 64 k point in the IBZ of the hexagonal lattice for YNi_4B. The total-energy calculations are performed with the experimental lattice parameters as well as with different reduced and extended volumes with the constant experimentally observed equilibrium c/a ratio for YNi_2B_2C and YRh_3B. We have calculated the total energy of the constituents in their stable structures to estimate the heat of formation of these compounds.

III. BAND STRUCTURE AND DENSITY OF STATES

A. YNi_2B_2C

1. Band structure

The band structure of YNi_2B_2C along the representative directions is shown in Fig. 2. The lowest band in Fig. 2 is derived from C $2s$ state and this is well separated from the bands which are participating in the conduction indicating that the carbon is not in the sp^3 hybridized state. Above the carbon $2s$ band in Fig. 2, there is a parabolic band mainly arising from the boron $2s$ states and this is also separated from the conduction states by a gap. The Fermi level is cut by the three bands (17, 18, 19th bands), which have mainly nickel $3d$ character with a small yttrium $4d$ character.

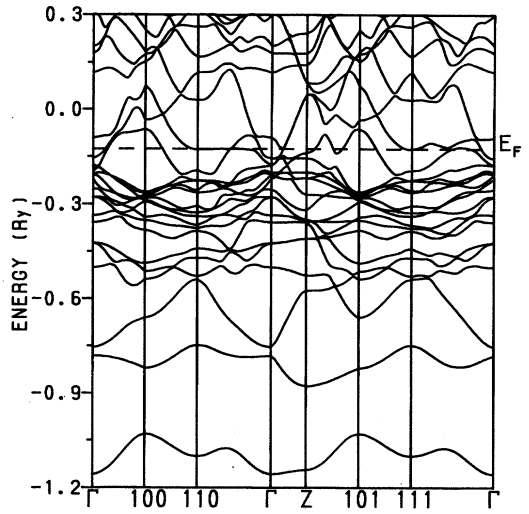

FIG. 2. Band structure of YNi_2B_2C.

Hence, it is expected that the electrons responsible for the conductivity are predominantly of d character of Ni and Y.

2. Role of key energy band in superconductivity

Even though the band structures of YNi_2B_2C and $LaPt_2B_2C$ appear to be similar, there is a subtle difference between the flat bands which exist in both systems along Γ-110 direction. The flat band (key energy band) in YNi_2B_2C is closer to E_F than that of $LaPt_2B_2C$. This may be one of the reasons for the system YNi_2B_2C to have higher T_c (15.6 K) than the other system (10 K). Whereas the band structures of $LuNi_2B_2C$ and YNi_2B_2C are quite similar to each other in all respects and hence, these systems possess nearly the same superconducting transition temperature.

It has been reported earlier that the position of a key energy band relative to E_F within the Ni-B-C sp manifold in RNi_2B_2C is sensitive to the NiB_4 tetrahedral geometry.[6] The neutron-diffraction studies on YNi_2B_2C show that its NiB_4 tetrahedral angle is 107.5° and this is closer to that of the ideal NiB_4 tetrahedron (109.5°).[31] Because of that, the geometry sensitive band is aligned closely with E_F. As discussed by Mattheiss *et al.*, due to the increase of atomic radius from Y to La, the corresponding NiB_4 tetrahedral angle is found to decrease as we go from YNi_2B_2C to $LaNi_2B_2C$ and as a consequence of that the key band, which almost coincides with the E_F in YNi_2B_2C, is well separated from E_F in $LaNi_2B_2C$.[6] As a result of this, the latter is found to be nonsuperconducting.[2] Due to the presence of layered structure, similar to the cuprate superconductors, one can expect two-dimensional nature in the band structure of this compound. But, because of the strong covalent interaction between constituents in all directions, the dispersion of bands along the c direction (i.e., in Γ-Z) is comparable to that in the plane (i.e., Γ-110) giving rise to a three-dimensional (3D) character. Because of the three-dimensional nature of the band structure, the single-crystal magnetization measurement of YNi_2B_2C shows the isotropic nature[32] which supports our band-structure inferences.

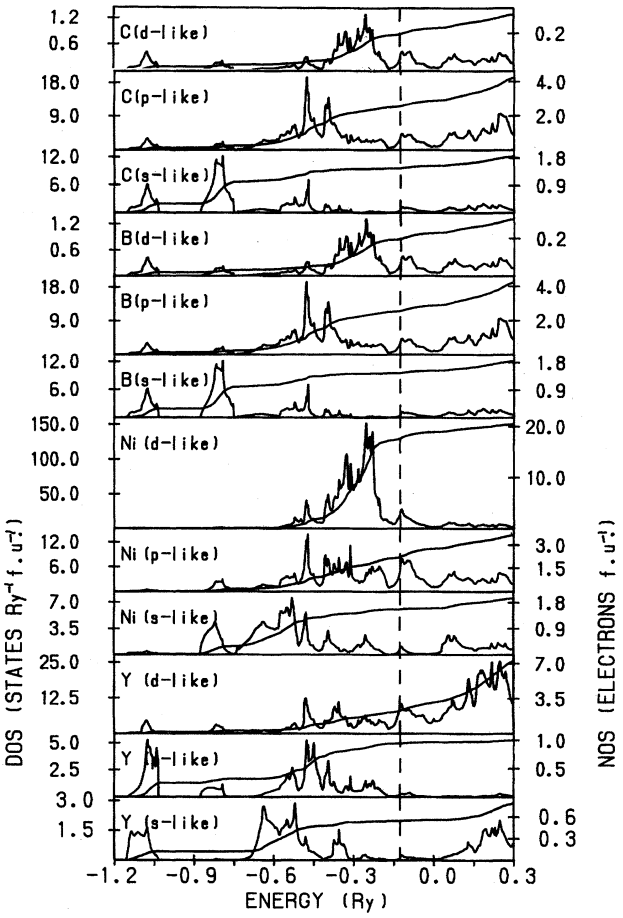

FIG. 3. Partial density of states of Y, Ni, B, and C in YNi_2B_2C.

3. Density of states

The partial density of states of YNi_2B_2C is shown in Fig. 3. The $N(E_F)$ is dominated by Ni d states and this is in agreement with the earlier theoretical[7,8] as well as the recent photoemission spectroscopy studies.[33] Due to the alignment of geometry sensitive flat band closer to the Fermi level, the E_F falls on the sharp peak in the density-of-states (DOS) curves in Fig. 4. The partial density of states (Fig. 3) clearly shows that the peak at the Fermi level arises from the states which are not confined to a single atomic layer and hence, these materials have a truly 3D character. The earlier band-structure studies on isostructural and isoelectronic $LaPt_2B_2C$ show that the E_F falls on the low-energy side of the peak in the DOS curve.[5] But in YNi_2B_2C, the E_F falls exactly on the sharp peak indicating that this may be one of the reasons for the latter to have higher T_c (15.6 K) than the former ($T_c = 10$ K). The topology of the DOS curve in the vicinity of E_F is very similar to that of the 16.6 K superconductor $LuNi_2B_2C$.[4,5] Moreover, the calculated value of $N(E_F)$ of YNi_2B_2C is closer to that of $LuNi_2B_2C$,[34] and this is consistent with the specific-heat measurements in the sense that the γ value of both compounds are almost the same.[15,23] The large density of states at Fermi level obtained

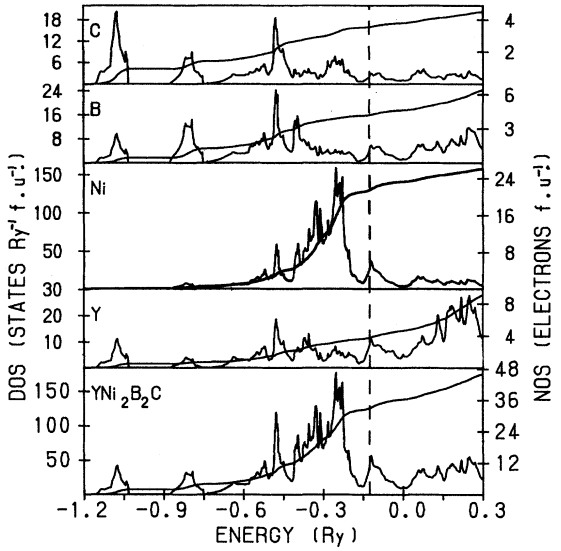

FIG. 4. Total density of states of YNi_2B_2C.

from our band-structure calculations is comparable with that of the $A15$ superconductors and this may be the probable reason for higher T_c.[34]

From the angular momentum and site decomposed DOS studies, we have found that the Ni $3d$ electron count (8.84 electron/atom) is almost similar to that of fcc nickel (8.61). Even though our observation contradicts the conclusions from specific-heat measurements by Hong *et al.*[23] who suggested a completely filled Ni $3d$ band in YNi_2B_2C, it is in agreement with x-ray photoemission spectroscopy[35] (XPS) studies, carrier density measurements,[36] and earlier band-structure calculations.[7,8]

4. Correlation effect

It is interesting to note that the experimental study shows the Ni d band is reduced by $\approx 20\%$ as a whole compared to the theoretical results and the measured spectra also show extra spectral weight around 5–10 eV below E_F.[37] Hence, the correlation effect plays a significant role in this material. The x-ray absorption spectroscopy studies on RNi_2B_2C systems also lead to the same conclusion.[35] The plasma energy obtained from band-structure calculations[5] is larger than the one obtained from the extended energy-loss spectroscopy[38] indicating that a considerable correlation effect exists in $R Ni_2B_2C$ compounds. The observed weak isotope effect[39] and the NMR measurement[40] also indicate the correlation effect in this material.

5. Chemical bonding

It is well established that the bonding nature of solids can be explained through band-structure calculations.[41] The Ni d states and the B p states are completely degenerate in the entire energy range in Fig. 3 indicating that there is a strong covalent bonding existing between Ni and B in YNi_2B_2C and this is consistent with the XPS study.[35] However, on account of more electronegative nature of C and B than Ni, the chemical bonding in YNi_2B_2C is of ionocovalent nature. Further, the partial DOS studies show that Y is not in the

TABLE I. The equilibrium lattice parameters (a_0,c_0 in Å), density of states at the Fermi level [$N(E_F)$ in states/(Ry f.u.)], Pauli paramagnetic susceptibility (χ_p in 10^{-6} emu/mol), electronic specific-heat coefficient (γ in mJ/mol K^2), electron-phonon coupling constant (λ), bulk modulus (B_0 in Kbar), pressure derivative of bulk modulus (B_0'), heat of formation (Δ_H in Kcal/mol) and cohesive energy (E_c KJ/mol) of superconducting YNi_2B_2C and YRh_3B and the nonsuperconducting YNi_4B.

	YNi_2B_2C		YRh_3B		YNi_4B	
Parameters	Expt.	Theo.	Expt.	Theo.	Expt.	Theo.
a_0	3.526	3.507	4.165	4.191	4.989	
c_0	10.542	10.485			6.953	
$N(E_F)$		43.87		53.66		74.71
χ_p	191.96	104.21	191.96	127.45	173.9	177.45
γ	18.2	7.61		9.31	14.1	12.96
λ	1.2	1.39				0.087
B_0		1.071		2.048		
B_0'		4.184		4.623		
Δ_H		−153.82		−129.56		+142.64
E_c		−4654.39		−4757.68		−4338.79

3^+ states in this compound and as a result all Y electrons are not transformed to C to form NaCl-type YC layers.

6. Evidence of peak at the Fermi level in the DOS curve

The following points support the existence of the peak at the Fermi level in the DOS curve of YNi_2B_2C. The experimental studies of Bud'ko *et al.* show that the substitution of Co, Fe, and Ru in the Ni site drastically decreases the T_c due to the shifting of the Fermi level.[42] The pressure variation of T_c of YNi_2B_2C has been correlated with the peak in the DOS near E_F, so that at high pressures the T_c is found to decrease with pressure.[43] The specific-heat and susceptibility measurements show that this material possesses large electronic specific-heat coefficient (γ) as well as Pauli paramagnetic susceptibility (χ_p).[23] As γ and χ_p are related to $N(E_F)$, the specific-heat and susceptibility measurements support the large value of $N(E_F)$ in this compound. In the rigid-band sense, when one substitutes Co or Cu in the Ni site, the E_F will shift to the lower or the higher-energy states of the DOS curve and as a consequence of that the $N(E_F)$ value will decrease if the E_F falls on the peak in YNi_2B_2C. Hence, the experimentally observed suppression of T_c by Co or Cu substitution in YNi_2B_2C (Ref. 44) supports our theoretical observation in the sense that the E_F falls on the peak. It is interesting to note that in the lower energy side of the E_F in the DOS curve (Fig. 4), the DOS drops sharply compared to the higher-energy side of the peak and this may be the reason for the T_c of the Co-doped system to decrease faster than the Cu-doped system.[44]

From the earlier studies on high-T_c $A15$ and $L1_2$ superconductors,[45,46] we have found that the E_F falls on a sharp peak of the DOS curve similar to YNi_2B_2C. Hence, we believe that this material is of the conventional BCS type rather than the strongly correlated type superconductor and this is in agreement with the recent tunneling and other experimental observations.[47,48] From our calculated and the experimental γ values, we have estimated the electron-phonon coupling constant (λ) using Eq. (2) and this is in good agreement with the experimental studies.[49] The calculated value of λ indicates that YNi_2B_2C is the strong-coupling conventional superconductor (Table I) and this is in support of the above viewpoint.

B. YRh_3B

The calculated band structure and the corresponding density of states of YRh_3B are shown in Figs. 5 and 6, respectively. A parabolic band is present in the bottom of the conduction band and this is mainly from the s states of boron. The B s-like bands are hybridized with the bands which are participating in the conductivity indicating that the boron is in the sp^2 hybridized state. The cluster of bands existing around −0.3 Ry arises mainly from Rh d states. Even though several bands are closer to the Fermi level, only two bands from Rh d states cross the Fermi level in most of the symmetry directions. The most important feature of the band structure is the presence of a narrow band along Z-Γ-X direction and this narrow band is aligned closer to the Fermi level which feature is reminiscent of the key energy band of YNi_2B_2C. Due to this narrow band only, the E_F falls on the

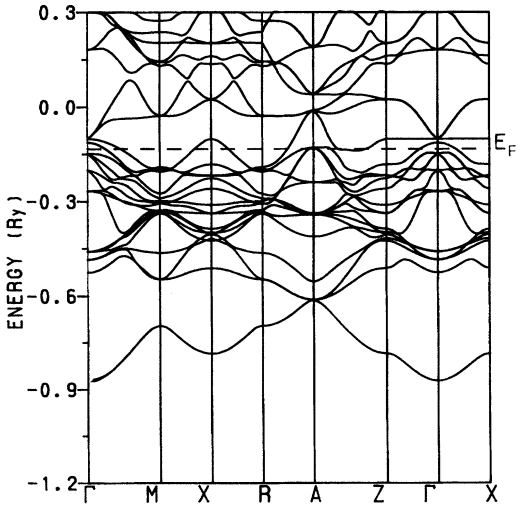

FIG. 5. Band structure of YRh_3B.

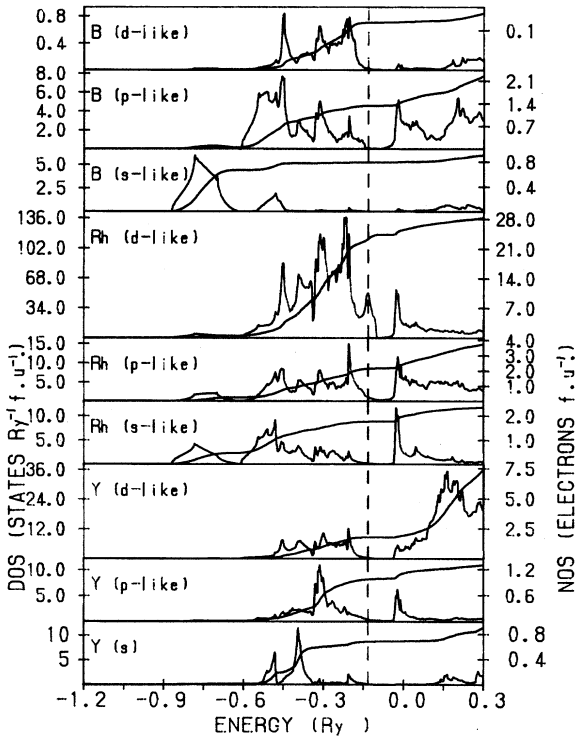

FIG. 6. Partial density of states of Y, Rh, and B in YRh_3B.

peak of the DOS curve in Fig. 6. We believe that similar to R Ni_2B_2C,[6] the T_c of YRh_3B can also be enhanced by making the system in such a way that this narrow band coincides with the Fermi level. The p states of B and the d states of Rh atoms are completely degenerate from the bottom of the conduction band to E_F in Fig. 6 indicating that there is a strong covalent bonding existing between B and Rh.

In all the perovskite-related oxides such as A_2MO_4 and AMO_3 (A=alkali, alkaline earth etc., M=transition metal), the MO_6 octahedra formed by the M-O bonds are believed to be important in understanding their properties.[30] Here also, we believe that the main electronic contribution for conductivity arises from BRh_6 octahedra and this will also be important for superconducting behavior of this material. Our site and angular momenta decomposed DOS in Fig. 6 clearly show that the electronic contribution to the conductivity arising from boron and yttrium sites is almost negligible and this indicates that the octahedrally distributed Rh atoms are important for superconductivity in this material. The Pauli paramagnetic susceptibility of YRh_3B obtained from our band-structure calculation is compared with the experimental value in Table I.[15] Surprisingly, the experimentally observed χ_p of both YRh_3B and YNi_2B_2C is the same (191.96×10^{-6} emu/mol) (Refs. 15 and 23) and this is consistent with our theoretical inference in the sense that the E_F falls in the vicinity of the peak of the DOS curves in both the compounds. The electronic specific-heat coefficient obtained from our band-structure calculation is given in Table I. Since the experimental g for this material is not available, we are unable to estimate the electron-phonon coupling constant of this material using Eq. (2).

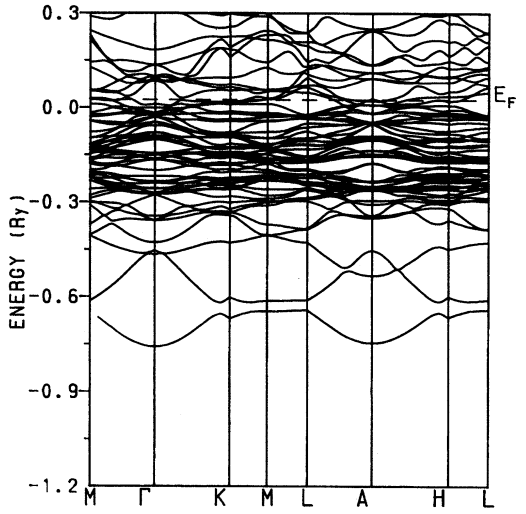

FIG. 7. Band structure of YNi_4B.

C. YNi_4B

In the band structure of YNi_4B shown in Fig. 7, a parabolic nature of band around -0.7 Ry arises from B s states and this is well separated from the conduction band. Above this, there are three broad bands, which hybridize with the conduction band, mainly having the s character of Y and Ni. The cluster of narrow bands from -0.3 to 0 Ry is mainly dominated by Ni $3d$ character and is considerably mixed with the Y d and B p states. The main peak in the DOS curve arises (Fig. 8) only due to these narrow bands. Even though the cluster of bands exists closer to the Fermi level, some broad bands cross the Fermi level in most of the symmetry directions and this is the reason for the falling of E_F on a valley after the main peak which is due to Ni d states in the DOS curve. Using the $N(E_F)$ value, the theoretical electronic specific-heat coefficient is calculated employing the following relation:

$$\gamma=\frac{\pi^2}{3}N(E_F)K_B^2. \tag{1}$$

From the experimental as well as theoretical γ values, the electron-phonon coupling constant (λ) can be obtained using the following relation:

$$\gamma_{\text{exp}}=\gamma_{\text{theo}}(1+\lambda). \tag{2}$$

The λ value obtained from the above relation given in Table I is almost negligible and is in agreement with the experimental studies that there is no superconductivity observed in pure YNi_4B.[23] But, though the calculated $N(E_F)$ of YNi_2B_2C is smaller than that of YNi_4B the experimentally observed γ value of YNi_2B_2C (18.2 mJ/mol K^2) is larger than that of YNi_4B (14.1 mJ/mol K^2) due to the electron-phonon mass-enhancement effect.[21] The Pauli paramagnetic susceptibility of YNi_4B obtained from our band-structure results is found to be in very good agreement with the experimental value (Table I).[23] The theoretically obtained χ_p values of YRh_3B and YNi_2B_2C are deviating much from the experimental values[15,23] (Table I) similar to our previous

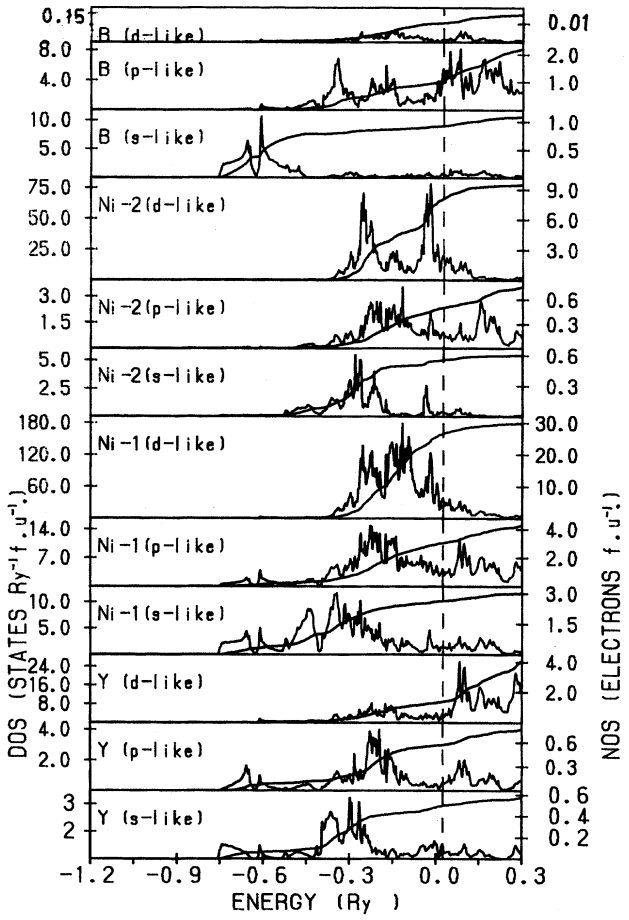

FIG. 8. Partial density of states of Y, Ni-1, Ni-2, and B in YNi_4B, where Ni-1 and Ni-2 represent the Ni atoms in two different equivalent positions $6i$ and $2d$, respectively.

studies on the $C15$ superconductors (ABi_2, A=K, Rb, Cs) (Ref. 50) and this may be related to the existence of superconductivity in these compounds.

The E_F falls on the DOS curve away from the main peak and this may be one of the reasons for this material to be paramagnetic even though the Ni d states are partially filled. From the partial DOS of YNi_4B, we have clearly found that the Ni d and the B p states are completely degenerate in the entire energy range of conduction band. This indicates that there is a strong covalent bonding existing between nickel and boron. Because of this strong covalent bonding, the Ni d states participate in the chemical bonding instead of exhibiting magnetism. The Ni atoms are in two distinct positions in YNi_4B and hence, the Ni d density of state arising from these two Ni sites is significantly different in Fig. 8. The integrated DOS up to E_F of the Ni $3d$ state in Ni($6i$) is 8.88 electron/atom and that in Ni($2d$) is 8.12, and these values are closer to that in fcc Ni (8.61), and this is contrary to the proposal of Hong *et al.* who suggested that the Ni $3d$ band is completely filled in YNi_4B.[20]

IV. TOTAL-ENERGY AND PHASE-STABILITY STUDIES

Using the site decomposed total-energy analysis, one can have an insight into the factors favoring the "good" sites or the "bad" sites for the structural stability.[51] With a potential of the atomic-sphere type and the electronic density $n(r)$ which is also approximated by the spherically averaged value, we obtain the following simple ASA expression for the total energy per cell of the valence electrons and the ions:

$$E_{\rm tot}=T_{\rm kin}+\sum_R U_R+\sum_R{}' \sum_{R'} Z_R Z_{R'} \times \sum_T |R-R'-T|^{-1}, \quad (3)$$

where the first term is the kinetic energy of the valence electrons which should be expressed as the difference between the total energy and the potential energy of the noninteracting electrons. In the ASA therefore,

$$T_{\rm kin}=\int^{E_F} EN(E)dE-\sum_R \int_0^{S_R} \nu_R(r) n_R(r) 4\pi r^2 dr, \quad (4)$$

where $N(E)=\Sigma_{Rl}N_{Rl}(E)$ is the sum of the projected DOS, $\nu_R(r)$ is the one-electron potential in the sphere at R and $n_R(r)$ is the spherically averaged charge density. The second term in Eq. (3) is the sum of the intrasphere interaction energy between the electrons themselves and between the electrons and the nucleus in that sphere and it can be expressed as

$$U_R\equiv\int_0^{S_R} n_R(r)\left[E_{xc}(n_R(r))-2Z_R r^{-1} + \int_0^{S_R} n_R(r')|r-r'|^{-1}4\pi r'^2 dr'\right]. \quad (5)$$

The third term in Eq. (3) is the intersphere Coulomb (or Medelung) energy. Here, Z_R is the difference between the nuclear charge and the electronic charge in the sphere at R. Equation (3) has proved useful for self-consistent calculations of the site decomposed total energies in the cell and we use it in this work to investigate the local picture of the structural energies.[52]

The site decomposed total energies of YNi_2B_2C, YRh_3B, and YNi_4B relative to that of their constituents in their elemental state are given in Table II. From the table, it is clear that the Y site is favorable for stability in all these three compounds. The introduction of carbon in YNi_4B forms a strong bonding between Y and C. As a result of this the favorable energy for stability arising from the Y site in YNi_2B_2C is larger than that in YNi_4B. The B site is a bad site in favoring the formation of these compounds in their

TABLE II. The site decomposed total-energy difference between the elemental and the compound state (Δ_E in Ry) of the constituents in YNi_2B_2C, YRh_3B, and YNi_4B.

YNi_2B_2C	Y	Ni	B	C
Δ_E	−0.926 989	−0.382 729	+0.196 526	+0.479 510
YRh_3B	Y	Rh	B	
Δ_E	−0.656 579	−0.091 359	+0.380 326	
YNi_4B	Y	Ni($6i$)	Ni($2d$)	B
Δ_E	−0.466 359	−0.047 789	+0.112 671	+0.695 076

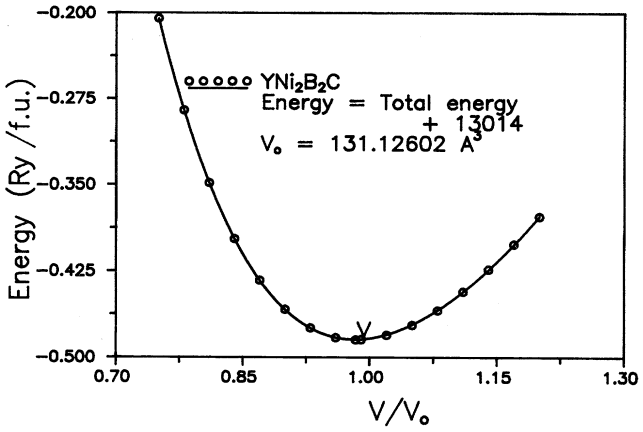

FIG. 9. Total energy as a function of volume in YNi_2B_2C.

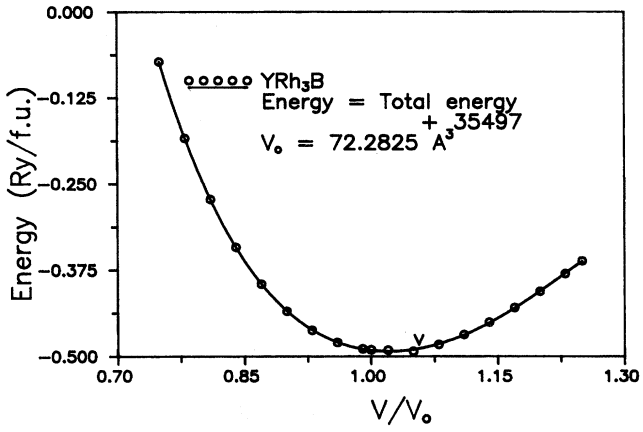

FIG. 10. Total energy as a function of volume in YRh_3B.

respective structures since it has a more positive energy than that calculated for the elemental boron. In YNi_2B_2C, the structural energy arising from the C site also is not favorable for stability. Yet, on the introduction of carbon, the Y site gains favorable energy and hence, the stable YNi_2B_2C compound is formed even though YNi_2B_2 is found to be unstable.[23] From Table II, it is clear that the Ni($6i$) and Ni($2d$) sites play opposite roles with respect to the stability of YNi_4B in the hexagonal $CeCo_4B$-type structure. The sum of favorable energy for stability arising from Y and Ni($6i$) sites is smaller than the sum of unfavorable energy for stability arising from Ni($2d$) and B sites. Because of the above fact, this system prefers superstructure.

From the difference between the total energy of the compound and the weighted sum of the total energy of the constituents, the values of heat of formation for all the three compounds are calculated and given in Table I. Among the three compounds, the heat of formation of YNi_4B is found to be positive indicating that this material is in the metastable state and this will form only by endothermic reactions. The positive value of ΔH of YNi_4B may be related to the formation of superstructure.[21] The negative values of ΔH of the superconducting compounds YNi_2B_2C and YRh_3B show that they are stable and this is consistent with the experimental studies.[23,15]

The total energy versus volume curves of YNi_2B_2C and YRh_3B are shown in Figs. 9 and 10, respectively. The equilibrium volumes are obtained from the energy minimum and from that, the calculated lattice parameters of these compounds are given in Table I. From the table, the calculated values of lattice parameters are within 0.6% of deviation from the experimental value indicating that the LDA is well described in the ground state of these materials.

The cohesive energy for all these three compounds is calculated from the difference between the total energy of the compounds and the weighted sum of the total energy of their constituents in their atomic states. From the cohesive energies given in Table I, we have found that the cohesive energy of YNi_4B is smaller than that of YNi_2B_2C. It is well known that the cohesive energy is an indirect measure of the bond strength of the solid and hence, we can expect the melting point of YNi_4B to be smaller than that of YNi_2B_2C and this is in good agreement with the experimental studies in the sense that the experimentally estimated θ_D of YNi_4B (458 K) is found to be smaller than that of YNi_2B_2C (537 K).[21] This lattice stiffening might be attributed to the carbon atoms which are considered to act as the bridging atoms between each set of two boron atoms thus forming a B-C-B unit thereby increasing the bonding within the B-Y-B subsystem.

V. EQUATION OF STATE STUDIES

Although different classes of solids exhibit different bonding natures, Vinet *et al.* have argued that under compression the pressure-volume relation is dominated by the overlap interaction for all the classes of solids. On account of this, the empirical evidence of applicability of the universal equation of state (UEOS) for different classes of solids has been demonstrated.[53] As the chemical bonding in our systems is in the mixed nature, the universal equation of state is appropriate for our EOS analysis. A universal binding-energy–distance relationship[54] of the form, $E(a)=\Delta E E^*(a^*)$, where $E^*(a^*)$ is the universal function of the scaled length a^* and Δ_E is the total energy at equilibrium. This universal energy relation leading to the universal equation of state[54] is put forth by Vinet *et al.* which is as follows:

$$P(V)=3B_0\left(\frac{1-X}{X^2}\right)e^{\eta(1-X)}. \tag{6}$$

The above expression accurately represents the P-V relation for all the classes of solids under compression, where $X=(V/V_0)^{1/3}$, B_0 is the isothermal bulk modulus, and V_0 is the equilibrium volume, $\eta=3[B_0'-1]/2$, and $B_0'=(dB/dP)_{P=0}$.

According to the theory of Vinet *et al.*, if one defines $H(x)$ as $X^2P(x)/3(1-x)$, then the $\ln[H(x)]$ versus $1-x$ curve should be nearly linear by

$$\ln[H(x)]\approx\ln B_0+\eta(1-x). \tag{7}$$

From the total-energy curves of YNi_2B_2C and YRh_3B (Figs. 9, 10), the pressures corresponding to the different volumes are generated from the following relation:

$$P(V)=-(dU/dV)_{T=0}, \tag{8}$$

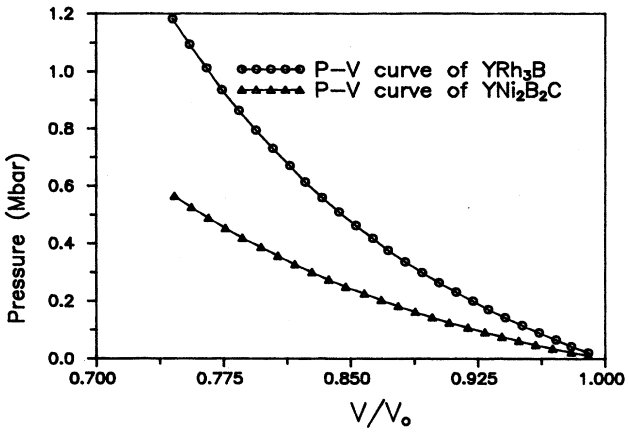

FIG. 11. Equation of state of YNi_2B_2C and YRh_3B.

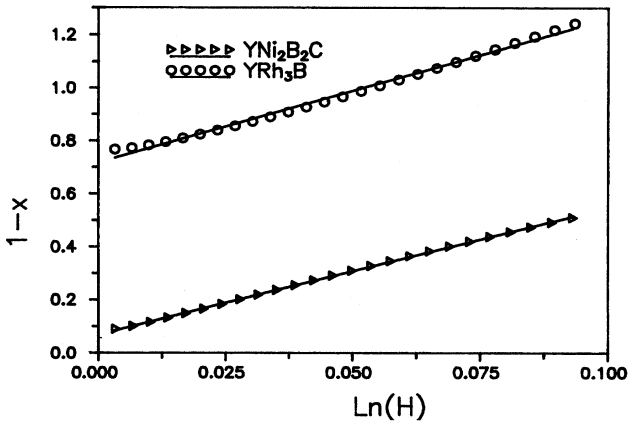

FIG. 12. The $\ln(H)$ vs $1-x$ curve of the superconducting YNi_2B_2C and YRh_3B.

and from this, the obtained pressure-volume curves for these compounds are shown in Fig. 11. From the figure, we have clearly found that the YRh_3B compound is less compressible compared to YNi_2B_2C. The possible reason for the low compressibility in YRh_3B may be due to the close-packed nature of its crystal structure. Using the P-V data, the $\ln[H(x)]$ and $1-x$ are generated for both the superconductors and a graph is plotted as in Fig. 12. Figure 12 exhibits excellent linearity in both the compounds indicating that the UEOS is more applicable for these compounds.[55] From Fig. 12, the intercept of YNi_2B_2C is lower than that of YRh_3B indicating that the bulk modulus of YNi_2B_2C is lower than that of YRh_3B and this may be due to its layered nature of crystal structure. From the intercept and slope of the linear curves in Fig. 12, the bulk modulus and its pressure derivative for these two compounds are obtained and given in Table I. The previously calculated values of bulk modulus of structural intermetallics using UEOS analysis show a good agreement with the corresponding experimental values,[56] whereas the experimental bulk modulus of YNi_2B_2C and YRh_3B are not available to confirm our results.

VI. CONCLUSIONS

(1) The E_F of both YRh_3B and YNi_2B_2C falls on the peak of their respective DOS curves and this is one of the causes for these systems to become superconductors.

(2) The octahedrally distributed Rh atoms in YRh_3B are mainly responsible for superconductivity in this compound.

(3) Due to the layered nature of the crystal structure of YNi_2B_2C, the calculated bulk modulus for this compound is less than that of YRh_3B which is in the close-packed structure.

(4) Our angular momentum and site decomposed DOS studies on YNi_4B and YNi_2B_2C show that the Ni-d states are partially filled. Even though this observation contradicts the proposal of Hong *et al.* this is conformable with the results obtained from the photoemission studies.

ACKNOWLEDGMENTS

The authors (P.R. and R.A.) are thankful to DAE, India and CSIR, India for their financial support. P.R. is indebted to Professor G. Baskaran, Institute of Mathmatical Science (IMSc), Madras for his encouragement to carry out this work. The authors are grateful to Dr. G. Subramoniam for his help in various stages. The computational facilities provided by the IMSc, Madras have been duly acknowledged.

[1] W. H. Lee, F. A. Yang, C. R. Shih, and H. D. Yang, Phys. Rev. B **50**, 6523 (1994); N. Sato, K. Imamura, T. Sakon, T. Komatsubara, I. Umehara, and K. Sato, J. Phys. Soc. Jpn. **63**, 2061 (1994); C. Mazumdar, K. Ghosh, S. Ramakrishnan, R. Nagarajan, L. C. Gupta, G. Chandra, B. D. Padalia, and R. Vijayaraghavan, Phys. Rev. B **50**, 13 879 (1994); C. Mazumdar, R. Nagarajan, C. Godart, L. C. Gupta, M. Latroche, S. K. Dhar, C. Levy-Clement, B. D. Padalia, and R. Vijayaraghavan, Physica B **194-196**, 1985 (1994); Solid State Commun. **87**, 413 (1993).

[2] R. J. Cava *et al.*, Nature (London) **367**, 252 (1994).

[3] R. J. Cava *et al.*, Nature (London) **367**, 146 (1994).

[4] L. F. Mattheiss, Phys. Rev. B **49**, 13 279 (1994).

[5] W. E. Pickett and D. J. Singh, Phys. Rev. Lett. **72**, 3702 (1994); D. J. Singh, Phys. Rev. B **50**, 6486 (1994).

[6] L. F. Mattheiss, T. Siegrist, and R. J. Cava, Solid State Commun. **91**, 587 (1994).

[7] R. J. Coehoorn, Physica C **228**, 331 (1994).

[8] J. I. Lee, T. S. Zhao, I. G. Kim, B. I. Min, and S. J. Youn, Phys. Rev. B **50**, 4030 (1994).

[9] J. L. Sarro, M. C. de Andrade, J. Hermann, S. H. Han, Z. Fisk, M. B. Mapple, and R. J. Cava, Physica C **229**, 65 (1994).

[10] K. A. Gschneidner, Jr., in *Science and Technology of Rare Earth Materials*, edited by E. C. Subbarao and W. E. Wallace (Academic, New York, 1980), p. 85; J. Alloys Compounds, **190**, 83 (1993).

[11] F. Heinigner, E. Bucher, J. P. Maita, and P. Descouts, Phys. Rev. B **8**, 3194 (1973).

[12] *Superconductivity in Ternary Compounds*, edited by M. B. Maple and O. Fisher (Springer-Verlag, Berlin, 1982), Vols. 1 and 2.
[13] J. M. Vandenberg and B. T. Matthias, Proc. Nat. Acad. Sci. USA **74**, 1336 (1977).
[14] D. C. Johnston, Solid State Commun. **24**, 699 (1977).
[15] H. Takei, N. Kobayashi, H. Yamauchi, T. Shishido, and T. Fukase, J. Less-Common Met. **125**, 233 (1986).
[16] P. Rigl and L. DeLong, J. Less-Common Met. **91**, 97 (1983).
[17] A. Schroder *et al.*, Phys. Rev. Lett. **72**, 136 (1994).
[18] C. Geibel *et al.*, Z. Phys. B **84**, 1 (1991).
[19] K. J. Strnat, in *Ferromagnetic Materials*, edited by E. P. Wohlfarth and K. H. J. Buschow (Elsevier, Amsterdam, 1988), Vol. 4, p. 131.
[20] N. M. Hong, N. P. Thuy, G. Schauly, T. Holubar, G. Hilscher, and J. J. M. France, J. Appl. Phys. **73**, 5698 (1993).
[21] N. M. Hong, T. Holubar, G. Hilscher, M. Vybornov, and P. Rogl (unpublished); G. Hilscher, H. Michor, N. M. Hong, T. Holubar, W. Perthold, M. Vybornov, and P. Rogl, Physcia B **206&207**, 542 (1995); G. Hilscher, T. Holubar, N. M. Hong, H. Michor, W. Perthold, M. Vybornov, and P. Rogl (unpublished).
[22] C. Mazumdar, R. Nagarajan, C. Godart, L. C. Gupta, M. Latroche, S. K. Dhar, C. Levy-Clement, B. D. Padalia, and R. Vijayaraghavan, Solid State Commun. **87**, 413 (1993).
[23] N. M. Hong, H. Michor, M. Vybornov, T. Holubar, P. Hundegger, W. Perthold, G. Hilscher, and P. Rogl, Physica C **227**, 85 (1994).
[24] T. Siegrist, H. W. Zandbergen, R. J. Cava, J. J. Krajewski, and W. F. Peck, Jr. Nature (London) **367**, 254 (1994).
[25] W. H. Butler, in *Treatise on Materials Science and Technology*, edited by Frank Y. Fradin (Academic, New York, 1981), Vol. 21, pp. 165–221.
[26] Yu. B. Kuz'ma and M. P. Khaburskaya, Izv. Akad. Nauk SSSR Neorg. Mater. **11**, 893 (1973).
[27] O. K. Andersen and O. Jepsen, Phys. Rev. Lett. **53**, 2571 (1984); O. K. Andersen, Z. Pawlowska, and O. Jepsen, Phys. Rev. B **34**, 5253 (1986).
[28] O. K. Andersen, *Electronic Structure of Complex Systems*, edited by P. Phariseau and W. M. Temmerman (Plenum, New York, 1984), p. 11; O. K. Andersen, Solid State Commun. **13**, 133 (1973).
[29] O. Jepsen and O. K. Andersen, Solid State Commun. **9**, 1763 (1971); P. Blochl, Ph.D. thesis, University of Stuttgart, 1989.
[30] J. B. Goodenough, in *Progress in Solid State Chemistry* (Pergamon, New York, 1977), Vol. 5.
[31] B. C. Chakoumakos and M. Paranthaman, Physica C **227**, 143 (1994).
[32] M. Xu, B. K. Cho, P. C. Canfield, D. K. Finnemore, and D. C. Johnston, Physica C **235-240**, 2533 (1994).
[33] M. S. Golden, M. Knupfer, M. Kielwein, M. Buchgeister, and J. Fing, Europhys. Lett. **28**, 369 (1995).
[34] S. A. Carter, B. Botlogg, R. J. Cava, J. J. Krajewski, W. F. Peck, Jr., and H. Takagi, Phys. Rev. B **50**, 4216 (1994).
[35] E. Pellegrin, G. Meigs, C. T. Chen, R. J. Cava, J. J. Krajewski, and W. F. Peck, Jr. (unpublished).
[36] X. X. Cywinski, Z. P. Han, R. Bewley, R. Cabitt, M. T. Wylie, E. M. Forgan, S. L. Lee, M. Warden, and S. H. Kilcoyne, Physica C **233**, 273 (1994).
[37] A. Fujimori, K. Kobayashi, T. Mizokawa, K. Mamiya, A. Sekiyama, H. Eissaki, H. Takagi, S. Uchida, R. J. Cava, J. J. Krajewski, and W. F. Peck, Jr., Phys. Rev. B **50**, 9660 (1994).
[38] K. Widder, D. Berner, A. Zibold, H. P. Geserich, M. Knupfer, M. Kielwein, M. Buchgeister, and J. Fink, Europhys. **30**, 55 (1995).
[39] D. D. Lawrie and J. P. Franck (unpublished).
[40] F. Borsa, Q. Hu, K. H. Kim, B. J. Suh, D. R. Torgeson, P. Canfield, M. Xu, and B. Zhong, Physica C **235-240**, 2547 (1994).
[41] R. Hoffmann, Rev. Mod. Phys. **60**, 601 (1988); C. D. Gellatt, Jr., A. R. Williams, and V. L. Moruzzi, Phys. Rev. B **27**, 2005 (1983).
[42] S. L. Bud'ko, M. Elmassalami, M. B. Fontes, J. Mondragon, W. Vanoni, B. Giordanenga, and E. M. Baggio-Saitovitch, Physica C **243**, 183 (1995).
[43] E. Alleno, J. Neumeier, J. D. Thompson, P. C. Canfield, and B. K. Cho, Physica C **242**, 169 (1995).
[44] A. K. Gangopadhyay, A. J. Schuetz, and J. S. Schilling (unpublished).
[45] P. Ravindran and R. Asokamani, Phys. Rev. B **50**, 668 (1994).
[46] P. Ravindran and R. Asokamani, J. Phys. Condensed Matter **7**, 5567 (1995).
[47] T. Ekino, H. Fuji, M. Kosuji, Y. Zenitani, and J. Akimitsu, Physica C **235-240**, 2229 (1994).
[48] R. Prozorov, E. R. Yacoby, I. Felner, and Y. Yeshurun, Physica C **233**, 367 (1994); M. Xu, P. C. Canfield, J. E. Ostenson, D. K. Finnemore, B. K. Cho, Z. R. Wang, and D. C. Johnston, *ibid.* **227**, 321 (1994); S. B. Roy, Zakir Hossain, A. K. Pradhan, C. Mazumdar, P. Chaddah, R. Nagarajan, C. Godart, and L. C. Gupta, Physica C **228**, 319 (1994).
[49] K. Wideter, D. Berner, A. Zibold, and H. P. Geserich (unpublished).
[50] S. Sankaralingam, S. Mathijaya, and R. Asokamani, J. Low Temp. Phys. **88**, 1 (1992).
[51] R. Phillips, H. Deng, A. E. Carlsson, and M. S. Daw, Phys. Rev. Lett. **67**, 3128 (1991); D. Nguyen Manh, A. Pasturel, A. T. Paxton, and M. van Schilfgaarde, J. Phys. Condens. Matter **6**, 2861 (1994).
[52] O. K. Andersen (unpublished).
[53] P. Vinet, J. H. Rose, J. Ferrante, and J. R. Smith, J. Phys. Condens. Matter **1**, 1941 (1989).
[54] P. Vinet, J. Ferrante, J. R. Smith, and J. H. Rose, J. Phys. C **19**, 9319 (1987); J. Phys. C **19**, 1467 (1986).
[55] De-Cheng Tian and Xiao-Bing Wang, J. Phys. Condens. Matter **4**, 8765 (1992).
[56] P. Ravindran, G. Subramoniam, and R. Asokamani, Phys. Rev. B (to be published).